This PDF contains the following sections:

Long-term effects of early postnatal stress on Sertoli cells functions

Kristina M. Thumfart[1,2], Samuel Lazzeri[1,2,#a,#b], Francesca Manuella[1,2], Isabelle M. Mansuy[1,2*]

[1]Laboratory of Neuroepigenetics, Institute for Neuroscience, Department of Health Sciences and Technology, ETH Zurich, Zurich, Switzerland

[2]Laboratory of Neuroepigenetics, Brain Research Institute, Medical Faculty of the University of Zurich, Zurich, Switzerland

[#a]Current address: IFOM, FIRC Institute of Molecular Oncology, Milan, Italy

[#b]Current address: University of Milan, Department of Oncology and Hemato-oncology, Milan, Italy

*Corresponding author

Email: imansuy@ethz.ch (IMM)

Abstract

Sertoli cells are somatic cells in testes essential for spermatogenesis, as they support the development, maturation, and differentiation of germ cells. Sertoli cells are metabolically highly active and physiologically regulated by external signals, particularly factors in the blood stream. In disease conditions, circulating pathological signals may affect Sertoli cells and consequentially, alter germ cells and fertility. While the effects of stress on reproductive cells have been well studied, how Sertoli cells respond to stress remains poorly characterized. Therefore, we used a mouse model of early postnatal stress to assess the effects of stress on Sertoli cells. We developed an improved enrichment strategy based on intracellular stainings and obtained enriched preparations of adult Sertoli cells from exposed males. We show that adult Sertoli cells have impaired electron transport chain (ETC) pathways and that several components of ETC complexes I, III, and IV are persistently affected. We identify the circulation as a potential mediator of the effects of stress, since treatment of primary Sertoli cells with serum from stressed males induces similar ETC alterations. These results newly highlight Sertoli cells as cellular targets of early life stress, and suggest that they may contribute to the negative effects of stress on fertility.

Keywords

Sertoli cell, adult testis, electron transport chain, mitochondria, early postnatal stress, mice

Graphical abstract

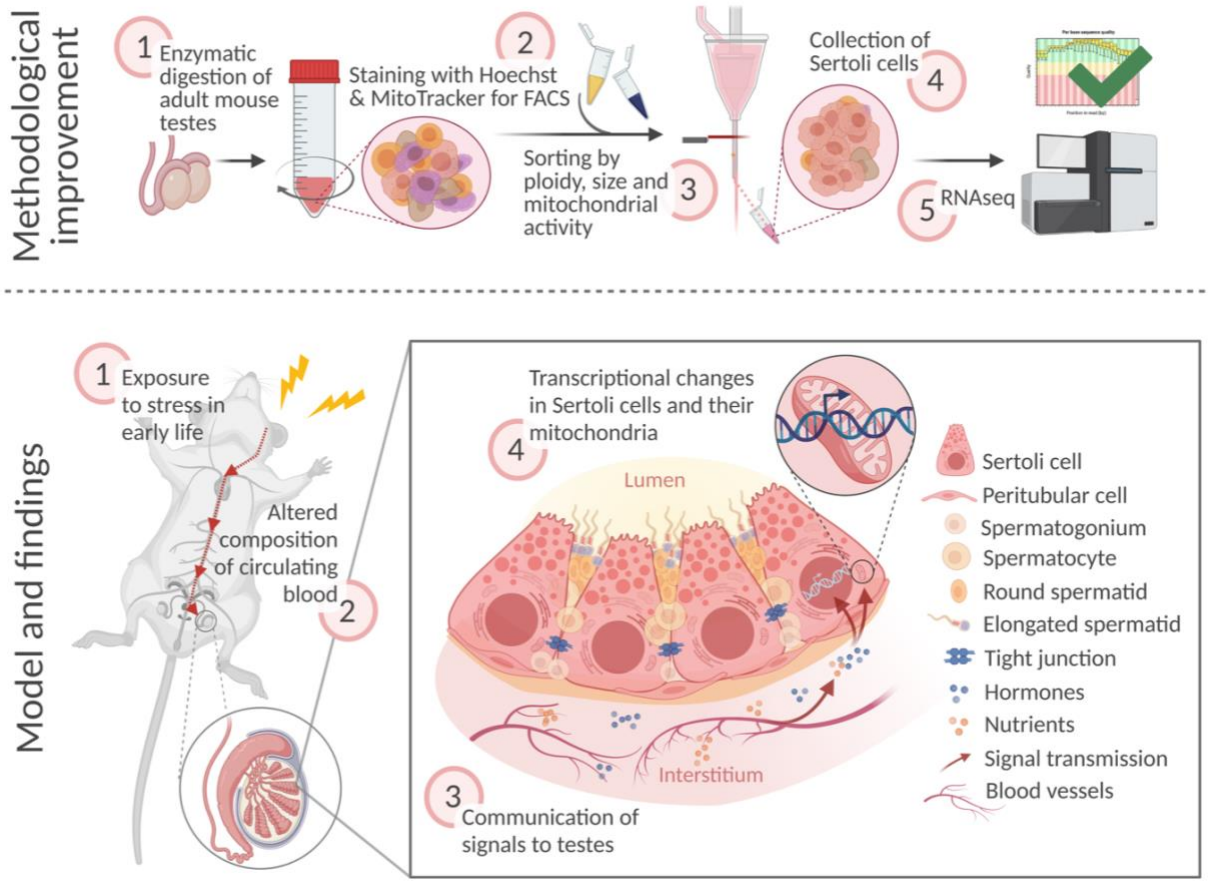

Highlights

- We present an improved method to obtain enriched preparations of Sertoli cells from adult mouse testis for molecular analyses
- Sertoli cells from adult males exposed to stress during early postnatal life have altered electron transport chain (ETC) expression, suggesting persistent effects of early life stress on Sertoli cells physiology
- Serum from adult males exposed to early postnatal stress reproduces ETC gene dysregulation in cultured Sertoli cells.

Introduction

Sertoli cells are somatic cells in the seminiferous tubules of testes tightly associated with germ cells and essential for spermatogenesis. They provide physical and structural support to differentiating spermatogenic cells and form and maintain a protective blood-testis barrier (Griswold 2018). Sertoli cells have paracrine functions and secrete growth factors, hormones, cytokines, and extracellular vesicles (Mancuso et al. 2018). These factors provide developmental guidance and immunological protection to germ cells (Mäkelä and Hobbs 2019; Kaur et al. 2020). Sertoli cells have a high glycolytic flux to provide nutritional support for germ cells. Through glycolysis, they metabolize glucose into lactate, which is the primary source of energy for spermatocytes and spermatids (Zhang et al. 2018). For their own energy needs, Sertoli cells rely on oxidative phosphorylation of lipids, which they receive through the blood stream or through the recycling of germ cell waste material (Regueira et al. 2018). Oxidative phosphorylation is catalyzed by four complexes of the electron transport chain (ETC) located in the mitochondrial inner membrane. These complexes use energy generated from nutrient oxidation to create a proton gradient across the mitochondrial inner membrane, which is then used by the ATP-synthase (complex V) to generate ATP (Nolfi-Donegan, Braganza, and Shiva 2020).

Sertoli cells are in close contact with blood vessels to sense hormones and metabolites present in the blood stream, and thereby receive signaling from circulating factors (Rebourcet et al. 2016). Changes in circulating factors in pathological conditions may therefore alter Sertoli cell metabolism and physiology and affect spermatogenic cells. This is particularly critical in early life, because Sertoli cells lose their mitotic activity during postnatal development and thus, if they are affected in early life, they are likely to remain so until adulthood (Sharpe et al. 2003). Indeed, altered blood homeostasis due to neonatal hormonal dysregulation in mice (Sarkar and Singh 2017) or early exposure to environmental toxins in rats (de Oliveira et al. 2020; Sadler-Riggleman et al. 2019) were shown to alter the energy metabolism of Sertoli cells. Exposure to high fat diet and resulting diabetes can also alter both glucose and lipid

metabolism of mouse Sertoli cells (Luo et al. 2020), which may contribute to altered reproductive functions in response to diabetes (Sajadi et al. 2019).

To gain insight into the effects of early life stress on Sertoli cells, we examined the transcriptome of Sertoli cells from adult males exposed to stress in early postnatal life using an improved method to enrich Sertoli cells from adult mouse testes. We observed that oxidative phosphorylation by the mitochondrial ETC is altered in adult Sertoli cells, and that many ETC components are affected. We further show that serum can recapitulate ETC components alterations in cultured Sertoli cells, suggesting the involvement of circulating factors in the alterations.

Results

Enrichment of Sertoli cells from adult testis

To obtain Sertoli cells from adult mouse testis, we developed an enrichment method based on fluorescence-activated cell sorting (FACS) not requiring any transgenic or surface marker (Fig 1a). First, testis tissue is digested sequentially in collagenase, trypsin and hyaluronidase (Bhushan et al. 2016), then cells are processed through FACS. While collagenase digests the interstitium and detaches seminiferous tubules from each other, trypsin fragments tubules and detaches peritubular cells. Hyaluronidase separates Sertoli cells from germ cells. The FACS strategy is based on intracellular staining with Hoechst and MitoTracker based on specific properties of Sertoli cells including diploidy (post-mitotic state) (Sharpe et al. 2003), large size (Wong and Khan 2021), and high metabolic activity compared to other cells in testes (Miettinen and Björklund 2017). Plotting of Hoechst intensity versus forward scatter (FSC), indicating size, identified several testicular subpopulations (Fig 1b). Diploid cells were separated from haploid (spermatids) and tetraploid (dividing) cells distinguished by Hoechst intensity (Fig 1c) (Gaysinskaya et al. 2014). Diploid cells were then fractionated by size using high and low FSC (Fig 1d), and cells of the high FSC fraction were separated into high and low MitoTracker

signal (high/low APC) for mitochondrial mass and activity (Fig 1e) (Clutton et al. 2019). Vimentin staining of single-cell suspension collected from seminiferous tubules before FACS identified 1.9 ± 0.6% (weighted mean ± weighted standard deviation) of Sertoli cells (Fig 1f) and after FACS, 14.8 ± 3.6% in the fraction of diploid cells (Fig 1g). This was further increased to 37.7 ± 30% in the high FSC cells fraction (Fig 1h) and up to 89.8 ± 5% in the fraction of cells with a high APC signal (Fig 1i).

Figure 1, Thumfart et al.

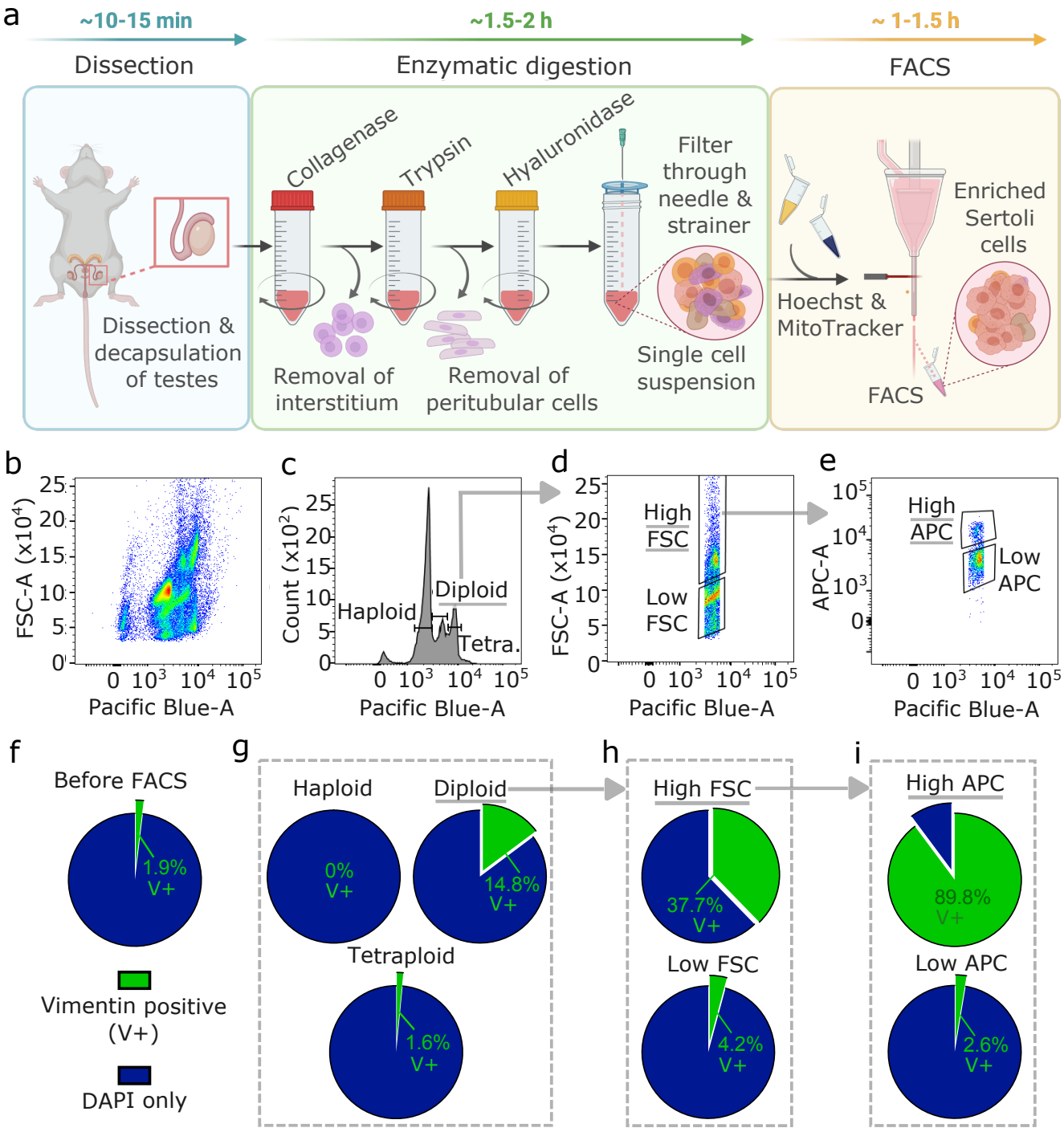

Fig 1. Sertoli cells enrichment and visualization by vimentin staining. (a) Workflow for Sertoli cells enrichment procedure including testis dissection, enzymatic digestion by collagenase, trypsin, and hyaluronidase, followed by staining with Hoechst and MitoTracker for FACS. Time estimates are indicated for the individual steps. (b-e) Results of FACS profiles during Sertoli cells enrichment. (b) Hoechst signal (Pacific Blue) plotted against FSC (indicating size) showing several cell populations in the single cell testis preparation. (c) Diploid cells selected using the Hoechst signal, (d) large cells using a high FSC signal, then (e) cells with high mitochondrial activity using MitoTracker (high APC) signal. (f-i) Enrichment of Sertoli cells (vimentin-positive, V+) in different FACS fractions. Percentage of V+ cells of all cells (DAPI) is shown (f) before FACS, (g) after selection of diploid cells, (h) after size selection by high FSC within diploid cells, and (i) after gating on high mitochondrial activity within diploid, high FSC cells (weighted averages of 4 independent replicates). Counts are summarized in S1 Table. Underlined fractions in (b-i) correspond to gates chosen for Sertoli cells enrichment. Arrows indicate implementation of gate settings before further partitioning into sub-gates.

Transcriptomic profiling of enriched Sertoli cells by RNA sequencing

We characterized the transcriptome of the Sertoli cells enriched from adult mouse testis by RNA sequencing and examined known markers of testicular cell populations using published single-cell sequencing datasets (Green et al. 2018). We observed that several Sertoli cell markers including *Amhr2, Clu, Ctsl, Rhox5,* and *Sox9* were more abundant in the isolated cells than markers of other testicular cells, validating the enrichment protocol (Fig 2a). The top 100 expressed genes were screened for enriched *Kyoto Encyclopedia of Genes and Genomes* (KEGG; Fig 2b) and *Gene Ontology* (GO; Fig 2c) pathways. Identified pathways involve immunological regulation, energy metabolism, cell-cell junctions, phagocytosis, and secretion, consistent with known Sertoli cell functions (Griswold 2018).

Figure 2, Thumfart et al.

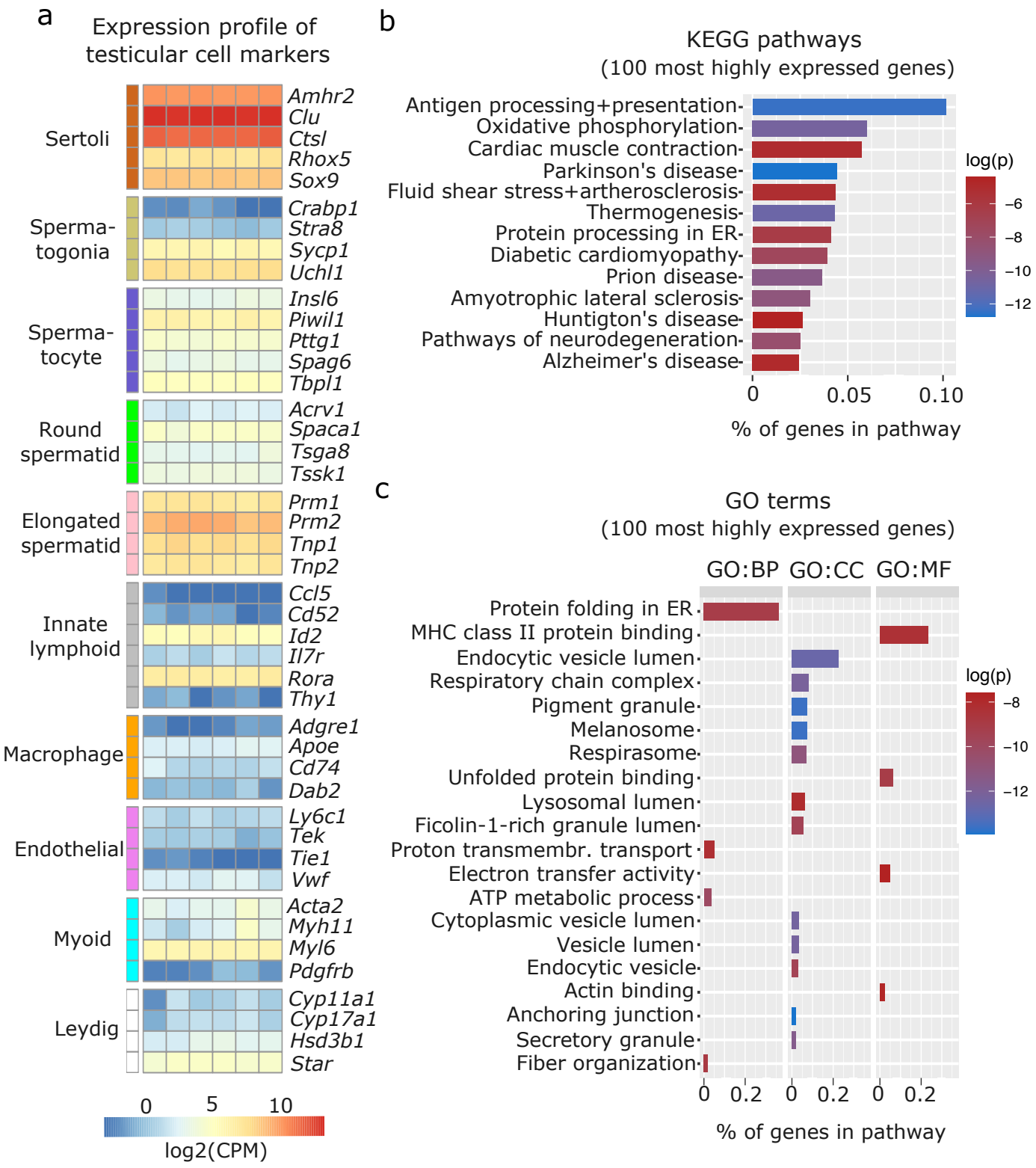

Fig 2. Characterization of enriched Sertoli cells by RNA sequencing. (a) Heatmap of testicular cell markers in enriched Sertoli cells, ordered by cell type-specificity including Sertoli cells, spermatogenic cells (spermatogonia, spermatocytes, round and elongated spermatids), immune cells (lymphoid and macrophage), endothelial cells, smooth muscle cells (peritubular myoid) and endocrine cells (Leydig). Color scale indicates normalized log2 gene counts per million (CPM). Enriched (b) KEGG and (c) GO pathways for 100 most highly expressed genes in collected Sertoli cells including immunological (e.g. KEGG: Antigen processing and presentation; GO MF: MHC class II protein binding), metabolic (e.g. KEGG: Oxidative phosphorylation, GO CC: respiratory chain complex), cell-cell junction (KEGG: Cardiac muscle contraction, GO, CC: anchoring junction), phagocytosis (GO, CC: endocytic vesicle lumen, lysosomal lumen), and secretion (KEGG: protein processing in ER, GO, CC: secretory granule) pathways. Ratio of genes per pathway is given on the x-axis and log of p-value (log(p)) is indicated on a color scale. BP: biological process, CC: cellular component, MF: molecular function.

Persistent changes in Sertoli cells transcriptome caused by early life stress

We used our improved enrichment method to obtain Sertoli cells from adult males exposed to stress in early postnatal life and examined the effects on the cells. As a stress paradigm, we used an established mouse model of postnatal stress based on unpredictable maternal separation combined with unpredictable maternal stress (MSUS) (Franklin et al. 2010). Newborn pups were separated from their mother unpredictably 3 hours each day from postnatal day 1 to 14 (PND1-14) and during separation, mothers were stressed unpredictably. This paradigm induces persistent metabolic and behavioral alterations in exposed animals when adult, and in their progeny across several generations (Gapp et al. 2014; Franklin et al. 2010). We collected Sertoli cells from adult MSUS and control mice from two independent cohorts (batch 1 and 2) and profiled their transcriptome by RNA sequencing in batch 1, followed by validation by quantitative PCR in batch 2 (Fig 3a). Using over-representation analyses of all genes with a p-value <0.05 from the RNA sequencing datasets, we observed that the most significantly altered molecular pathways (top five) were related to the mitochondrial ETC (S2 Table). Among KEGG pathways, “oxidative phosphorylation” ($p<0.001$) was the most significant (Fig 3b), while among GO terms for cellular components, “respirasome” ($p<0.001$) and “respiratory chain” ($p<0.001$) were the most significantly enriched (S1a Fig). To visualize ETC gene expression compared to the general expression distribution of all genes in the RNA sequencing datasets, we plotted candidates of the “oxidative phosphorylation” pathway with a p-value of <0.05 for control Sertoli cells (Fig 3c). All ETC components are more highly expressed than the average gene in Sertoli cells. Genes encoded by mitochondrial DNA (*ND2, ND4, ND6, CYTB, COX1, COX2*) have higher, but more variable expression than genes encoded by nuclear DNA (Fig 3c). This is consistent with recent single-cell RNA sequencing datasets in mouse testis (Green et al. 2018). In Sertoli cells from MSUS males, ETC genes encoded by nuclear DNA were primarily downregulated

compared to controls (Fig 3d), while changes in mitochondrial genes were more variable (S2a Fig). Validation of changes in ETC genes in a second batch of Sertoli cells by multiplex RT-qPCR screen (Fluidigm) confirmed that the majority of ETC genes were downregulated in MSUS Sertoli cells (Fig 3e). Out of 18 target genes identified from the KEGG pathway "oxidative phosphorylation", 4 were downregulated significantly ($p<0.05$; *ND4, ND6, CYTB*, *Uqcr11*), while no genes were significantly upregulated. When looking closer at downregulated genes, particularly components of ETC complex I, III, and IV were downregulated, while components of complex II and V had variable expression changes. Also, mitochondrial genes were predominantly downregulated, which was different to what we expected from the RNA sequencing data of batch 1, which showed higher inconsistency in mitochondrial gene expression changes (S2a Fig). However, this bias might be attributable to significant mitochondrial copy number variation (CNV) in MSUS vs. control Sertoli cell samples of batch 1 (S2b Fig).

Figure 3, Thumiart et al.

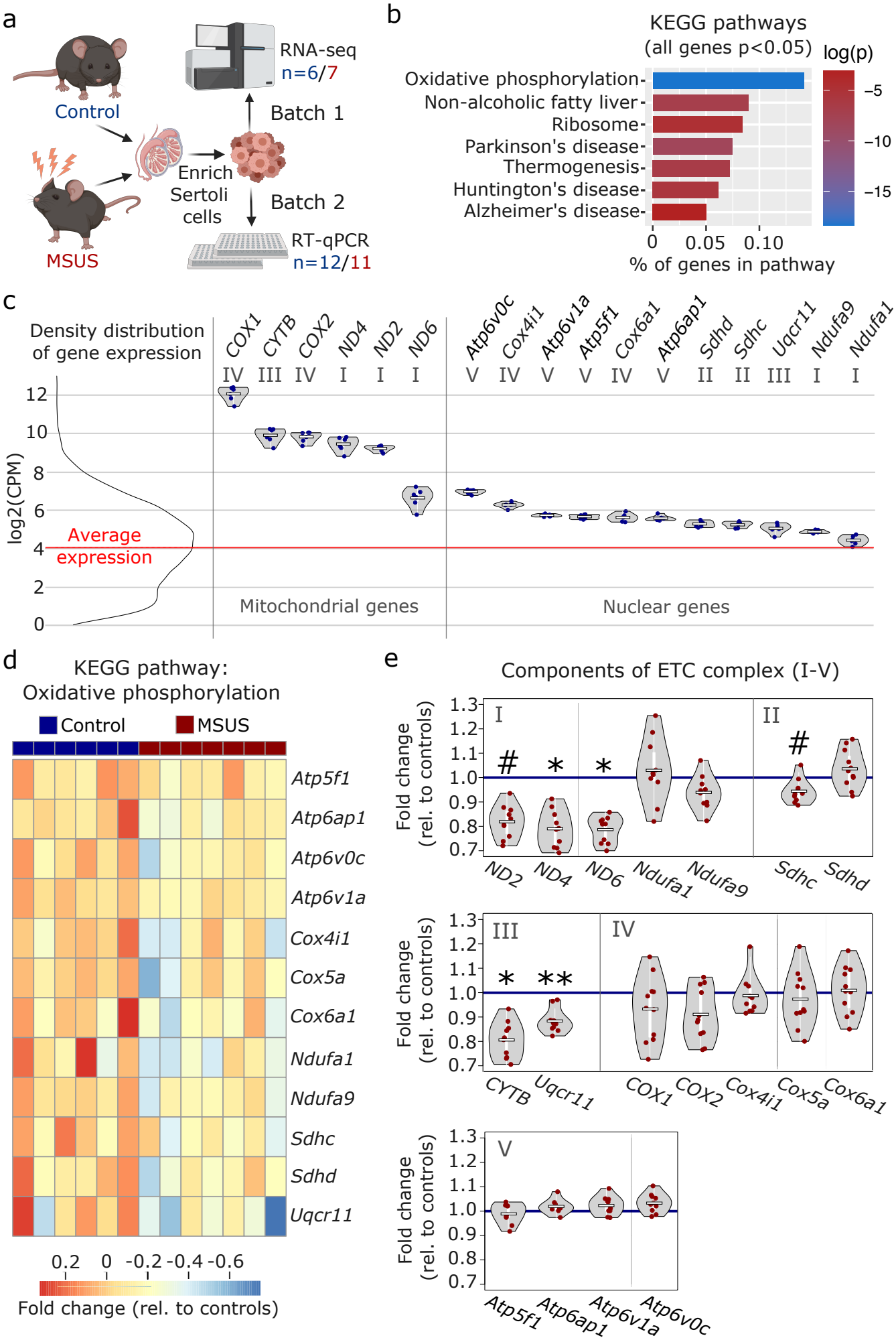

194 **Fig 3. Transcriptomic analyses of MSUS and control adult Sertoli cells.** (a) Schematic
195 representation of the experimental strategy for Sertoli cells enrichment and transcriptomic
196 analyses for control (blue) and MSUS (red) mice. For RNA sequencing, n=6 controls and n=7
197 MSUS (Batch 1). For validation of candidate genes with RT-qPCR, n=12 controls and n=11
198 MSUS (Batch 2). (b) KEGG pathways of significantly altered genes ($p<0.05$) in Sertoli cells
199 from MSUS males with % genes per pathway (x axis) and log of p-value (log(p)) on vertical
200 color scale. (c) Expression profile of ETC candidate genes from KEGG pathway "oxidative
201 phosphorylation" in control samples (scale is in log2(CPM)). Left, density distribution of all
202 expressed genes, with red line indicating the average expression of genes in control Sertoli
203 cells. Right, candidate genes encoded by mitochondrial (Mitochondrial genes) and nuclear
204 (Nuclear genes) DNA plotted on the same scale. Roman numbers indicate name of ETC
205 complex. Mean of control samples depicted as white line, individual samples as blue dots. (d)
206 Heatmap of nuclear encoded genes with $p<0.05$ of KEGG pathway "oxidative
207 phosphorylation". Fold change relative to controls is indicated in the color scale. (e) RT-qPCR
208 of ETC candidate genes in batch 2 samples. Candidate genes are divided according to ETC
209 complexes (I, II, III, IV, V) and fold change of expression profiles is shown for MSUS samples
210 relative to control mean (blue line) of respective genes. Mean of MSUS samples depicted as
211 white line, individual samples as red dots. $^{**}p<0.01$, $^{*}p<0.05$, #$p<0.1$, student's t-test.

212

Serum from MSUS males downregulates ETC components in primary Sertoli cells

Our previous work showed that serum from MSUS males can induce molecular changes in reproductive cells, when injected intravenously to adult males or when used to treat immortalized spermatogonial stem cells (van Steenwyk et al. 2020). Since Sertoli cells receive signals from the blood stream, we examined if serum from MSUS males can reproduce changes in ETC components observed after MSUS. We prepared primary Sertoli cell cultures from mouse testis and supplemented them with 10% serum obtained from MSUS or control mice for 24 hours (Fig 4a). Analyses of candidate genes by RT-qPCR showed that 4 ETC components are significantly downregulated ($p<0.05$; *ND6, Ndufa1, COX1, Cox6a*) (Fig 4b). Downregulation was most consistent for components of complex I, III, and IV while complex II and V components were more variably altered, and some of them upregulated ($p<0.05$; *Sdhc, Atp6ap1*).

Figure 4, Thumfart et al.

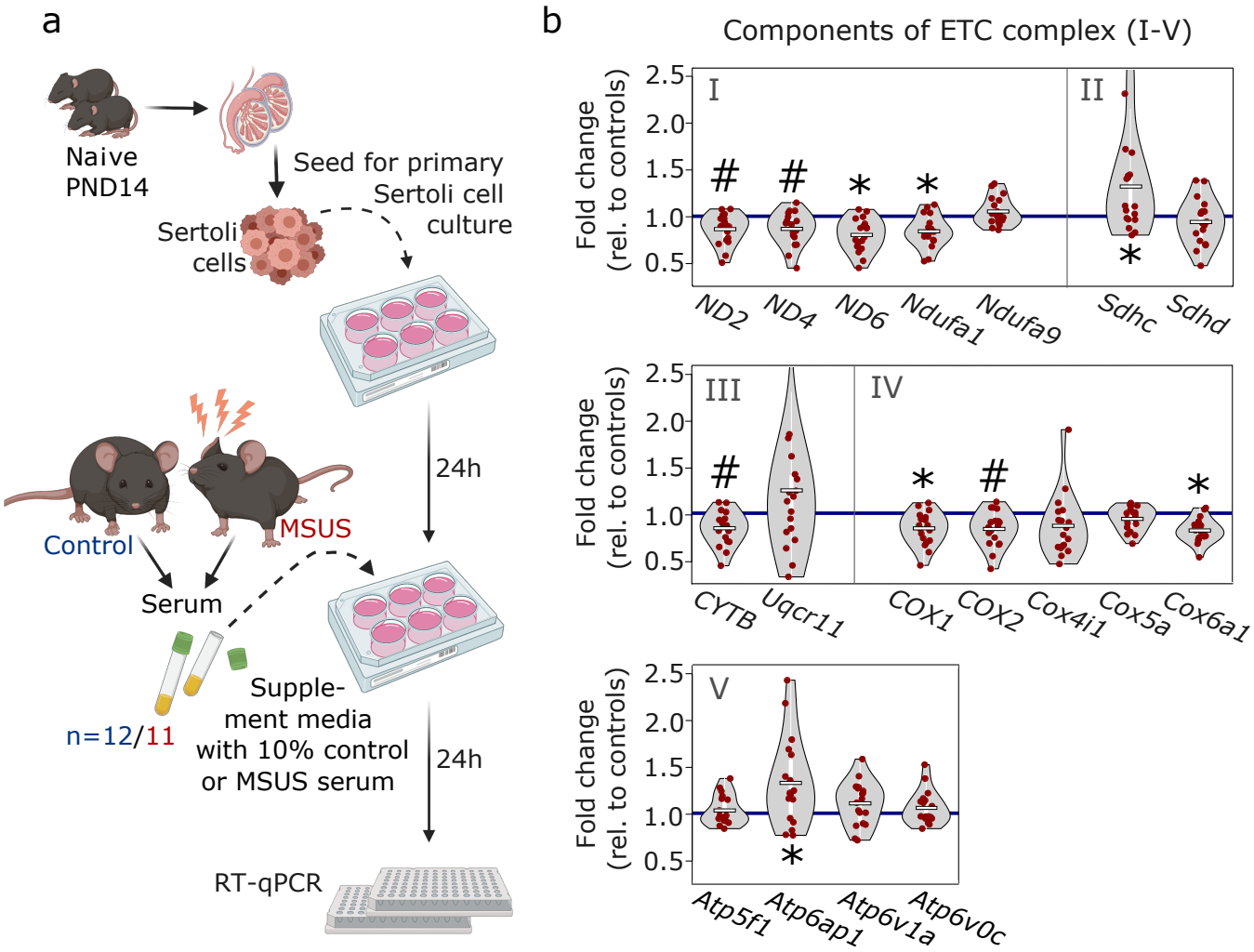

Fig 4. Analyses of ETC genes in primary Sertoli cells after MSUS serum exposure. (a) Schematic representation of the experimental strategy for serum treatment of Sertoli cells. Primary Sertoli cells from naïve mouse pups (PND14) were seeded and treated with 10% serum from control (blue) and MSUS (red) mice for 24h. Treated cells were then harvested for RT-qPCR. Controls, n=12; MSUS, n=11. Experiment was performed in duplicates. (b) RT-qPCR of ETC candidate genes in serum treated Sertoli cells. Candidate genes are divided according to ETC complexes (I, II, III, IV, V) and fold change of expression profiles is shown for MSUS samples relative to control mean (blue line) of respective genes. Mean of MSUS samples depicted as white line, individual samples as red dots. *p<0.05, #p<0.1, Kenward Roger method.

Exposure to MSUS serum does not alter metabolic functions of primary Sertoli cells

Differential regulation of the ETC can affect the intracellular redox state of cells and alter their lactate-pyruvate ratio (Titov et al. 2016; Patgiri et al. 2020). Therefore, we examined if the downregulation of ETC complex I, III, and IV components has metabolic consequences for Sertoli cells. We measured lactate and pyruvate in the conditioned medium of primary Sertoli cells after MSUS serum treatment and examined ROS activity by 2',7'–dichlorofluorescin diacetate (DCFDA) staining. The level of lactate and pyruvate was not significantly altered (S3a,b Fig). Likewise, the ratio of lactate to pyruvate (S3c Fig) or ROS levels (S3d Fig) were not altered. These results suggest that the downregulation of ETC complexes I, III, and IV after MSUS serum exposure was not sufficient to affect metabolic functions of Sertoli cells.

Discussion

This study examines the effects of early life stress on somatic cells in the adult mouse testis and addresses the question of which factors may play a role in the induction of these effects. Using an established mouse model of stress, we show that Sertoli cells from adult males exposed to stress in early postnatal life have altered ETC pathways. The alterations affect several mitochondrial complex components, which are predominantly downregulated in adult Sertoli cells. We link these alterations to circulating blood factors by showing that the ETC complexes downregulation can be reproduced in primary Sertoli cells in culture when the cells are treated with serum from exposed adult males. These results suggest that Sertoli cells can be persistently altered by adverse conditions in early life and keep a biological trace of exposure for many months. This may be explained by the fact that these cells are post-mitotic in the adult testis and are no longer able to self-renew unlike spermatogenic cells. They therefore do not have the possibility to correct or erase molecular changes by cell division and

264 renewal, and remain altered until adulthood, possibly throughout life. Other environmental
265 factors such as endocrine disruptors have also been found to affect Sertoli cells in rats
266 (Guerrero-Bosagna et al. 2013).

267 Since Sertoli cells are essential for germ cell maintenance and physiology, their persistent
268 alterations during development through to adulthood may affect spermatogenesis and have
269 detrimental consequences for germ cells and fertility. Psychological stress has indeed been
270 reported to reduce fertility in humans (Bräuner et al. 2020) and is known to lead to molecular
271 changes in spermatogenic cells in testis (Tian et al. 2021) and adult sperm in rodents (Gapp
272 et al. 2014; Franklin et al. 2010), with the potential to impair metabolism and behavior in the
273 offspring (Gapp et al. 2014). However, the mechanisms by which Sertoli cells may alter germ
274 cells are not known.

275 Our data that ETC components in Sertoli cells are affected, suggest a link between stress
276 exposure at a young age and mitochondrial functions in the adult. Mitochondria are organelles
277 known for their ability to adjust to changes in metabolic demand in cells (Bereiter-Hahn and
278 Vöth 1994). Thus, they are sensitive targets of systemic cellular perturbations and potential
279 sensors of environmental exposure. Indeed, ETC components in brain and muscle have
280 already been shown to be altered by early postnatal stress in mice (Ruigrok et al. 2021). Our
281 data extend these findings by showing that ETC complexes are also affected persistently in
282 Sertoli cells by early postnatal stress, and provide candidate molecular targets to examine in
283 relation to potential germ cell damage. The downregulated complexes I, III, and IV have in
284 common to be able to transport protons across the inner mitochondrial membrane, and
285 contribute to the generation of a proton gradient for ATP production (Marreiros et al. 2016).
286 This could influence the metabolism of not only Sertoli cells, but also of neighboring germ cells
287 via altered extracellular signaling pathways such as redox state and lactate production (Titov
288 et al. 2016; Patgiri et al. 2020). However, in cultured Sertoli cells, reproducing ETC pathways
289 alterations with serum from stressed males did not affect reactive oxygen species (ROS),
290 lactate or pyruvate level. This suggests that changes may only be subtle and cannot be

detected by classical methods such as fluorescent assays *in vitro*, or may be compensated for by alternative mechanisms. Using sensitive substrate sensors such as genetically encoded fluorescence resonance energy transfer (FRET) sensors to detect metabolite flows *in vitro* or *in vivo* may help identify changes (Mächler et al. 2016). Other systemic effects by cell-cell-communication within testis or signaling through innervation and via the lymphatic system may also occur.

Classically, methods to enrich Sertoli cells are based on specific culture procedures and conditions which have some limitations. For instance, *Datura stramonium* (DSA)-lectin coated dishes can be used to favor the attachment of Sertoli cells (Scarpino et al. 1998) and allow easier removal of contaminating germ cells by washing and/or hypotonic shock (Wagle et al. 1986; Anway et al. 2003). However, culture conditions can introduce biases to cells and modify their epigenetic landscape and functions compared to *in vivo* (Zomer and Reddi 2020a). Therefore, enrichment methods not requiring any culture, but allowing to isolate cells directly from tissue, are advantageous for molecular analyses. For Sertoli cells, transgenic or knock-in mice expressing fluorescent proteins under the control of *Amh* or *Sox9* promoters have been generated and can yield relatively pure Sertoli cell preparations by FACS (Zimmermann et al. 2015; Zomer and Reddi 2020b). However, wildtype mice may be preferable to avoid possible transgene interference (in homozygous mice for instance) or GFP protein toxicity, and for easier availability without requiring any specific breeding scheme. This is particularly needed for large-scale *in vivo* experiments that require big cohorts for phenotyping like behavioral, physiological and/or metabolic testing. Our FACS-based method provides an efficient alternative through capitalizing on previous work in fixed cells (Rotgers et al. 2015), using parameters that separate testicular populations by ploidy through DNA staining and light scattering via cytometry. Due to intracellular stainings with Hoechst and MitoTracker, biases due to cleavage or internalization of surface antigens after enzymatic digestion can be avoided (Autengruber et al. 2012; Tsuji et al. 2017). Using this method, we obtain a high enrichment of Sertoli cells confirmed by vimentin staining (Fig 1 f-i) and specific markers expression in

obtained cells (Fig 2a). Notably, markers of elongated spermatids such as *Prm2* were detected in our Sertoli cells datasets, similarly to previously reported in testis single-cell sequencing datasets (Green et al. 2018). These marker transcripts likely correspond to remnants of spermatids phagocytosed by Sertoli cells that persist in their cytoplasm. Lastly, we cannot exclude that Hoechst and MitoTracker binding affects DNA and mitochondria integrity in sorted Sertoli cells. However, incubation with the stains is kept to a minimum and cells are placed on ice at all times after staining.

In conclusion, our findings highlight the vulnerability of Sertoli cells during postnatal development and the fact that they can be persistently altered by stress exposure. Whether and how this may ultimately affect germ cells functions and physiology is still an open question that needs to be investigated.

Methods

Animals

Adult C57Bl/6J mice (3-5 months old) were kept under a 12-h reverse light/dark cycle in a temperature- and humidity-controlled facility with access to food and water ad libitum. All experiments were performed during the active (dark) cycle of the mice in accordance with guidelines and regulations of the Cantonal Veterinary Office, Zürich (animal licenses ZH057/15 and ZH083/18).

MSUS paradigm

3-month old female and male breeders were randomly paired and assigned to MSUS or control groups. Newborn pups in the MSUS group were separated from their mother for 3 h per day at unpredictable times from postnatal day (PND) 1 to 14. Any time during separation, mothers underwent an unpredictable acute swim in cold water (18°C for 5 min) or 20-min restraint in a tube. Control animals were left undisturbed. Pups were weaned at PND21 and

assigned to new cages according to group and gender (3–5 mice/cage). Siblings were assigned to different cages to avoid litter effects. An overview of MSUS and control mice used for tissue collection is presented in S3 Table.

Testis collection

Adult mice were single-housed with food and water *ad libitum* the night before sacrifice to minimize stress. Mice were sedated with isoflurane before decapitation. For testis collection in pups at PND14, whole litters (4-6 males on average) were sacrificed by decapitation soon after being removed from their mother.

Enzymatic digestion of mouse testis

Testes were dissected, decapsulated and placed into a 50 ml canonic tube containing 10 ml of enriched DMEM/F12 medium (1x DMEM/F12 [Gibco], supplemented with 15mM HEPES, 1x GlutaMAX [Gibco], 1x Minimum Essential Medium Non-essential Amino Acids [Gibco] and 1% penicillin-streptomycin [Pen-Strep; Gibco, 10,000 U/ml]). The tissue was transferred to 5 ml collagenase solution (1mg/ml collagenase [from Clostridium histolyticum, Sigma Aldrich] and 0.02 mg/ml DNase [from bovine pancreas, Sigma Aldrich] in enriched DMEM/F12) and incubated at 35°C for 5-10 minutes with intermittent shaking until seminiferous tubules dissociated from the interstitium. For washing, 25 ml of enriched DMEM/F12 were added, the tube was inverted three times and tubules were allowed to settle for 2-3 minutes. Supernatant containing interstitial cells was discarded and the washing step was repeated twice. Then, 5 ml 0.25% trypsin-EDTA solution (Gibco) supplemented with 0.1 mg/ml DNase were added to the tubules and incubated at 35°C for 5-10 minutes with intermittent shaking until tubules were fragmented. Tubules were washed one time with enriched DMEM/F12 containing 10% fetal bovine serum (FBS; HyClone, Cat. No. SV30160.03) to inactivate trypsin and were allowed to settle for 5 minutes. Supernatant containing peritubular cells was removed and washing was repeated with enriched DMEM/F12 two more times. To obtain a single-cell suspension from the cleaned seminiferous tubules, the tissue was further digested in hyaluronidase solution

(1mg/ml hyaluronidase [from sheep testes, Sigma Aldrich] and 0.02 mg/ml DNase in enriched DMEM/F12) for 5-10 more minutes at 35°C with intermittent shaking. For proper dissociation of cells, they were passed through a 5 ml serological pipette 4-5 times, then 25 ml enriched DMEM/F12 were added. Cells were centrifuged at 400xg for 3 minutes, the supernatant was removed and cells were resuspended in 10 ml enriched DMEM/F12. To remove any remaining cell clumps, the cell suspension was slowly passed through a 20G needle, then filtered through a 70 µm cell strainer. 25 ml of enriched DMEM/F12 were added and cells were centrifuged at 400xg for 3 minutes and collected for further enrichment.

Blood processing

To obtain serum, trunk blood was collected and allowed to clot for 15-30 minutes at room temperature (RT). To separate serum from the clot, samples were centrifuged for 10 minutes at 2,000 x g. The supernatant (serum) was transferred to a new tube and stored at -80°C until further use.

Fluorescence-activated cell sorting (FACS)

Cells obtained after enzymatic digestion of testis were resuspended in 5-10 ml FACS buffer (1x DPBS [Gibco] supplemented with 1% Pen-Strep, 1% FBS, 10 mm HEPES, 1 mm pyruvate [Gibco] and 1 mg/ml glucose [Gibco]) and counted with a hemocytometer. Cells were diluted at 10^6/100 µl in FACS buffer. 1 µl of Hoechst 33342 Solution (BDPharmingen, stock: 1 mg/ml) and 0.1 µl of MitoTracker Deep Red (Invitrogen, stock: 1mM) were added per 100 µl cell suspension, then cells were incubated at 35°C for 20 minutes. Thereafter, cells were kept on ice at all times. Cells were washed twice with ice-cold FACS buffer and the Sertoli cell fraction was sorted according to the FACS diagram depicted in Fig 1b-e. Briefly, cell debris and doublets were gated out and remaining cells were gated for diploidy using the Hoechst channel. Diploid cells were further gated for high FSC and subsequently for a high signal in the MitoTracker channel.

Immunocytochemistry

Round coverslips (diameter: 8mm, thickness: 1, Warner Instruments) were placed into 48-well plates and coated with Poly-L-lysin solution (P8920, Sigma-Aldrich) for at least 15 min at RT. Coverslips were then washed three times with distilled, autoclaved water and were allowed to dry overnight. The day after, always 40,000 cells in enriched DMEM/F12 medium supplemented with 10% FBS were plated onto the slides and allowed to attach at RT for at least 20 min and another hour in an incubator at 37°C. Thereafter, medium was aspirated and cells were fixed with 4% paraformaldehyde (PFA) for 15 min at RT. Cells were washed with PBS three times and then incubated in blocking solution (PBS supplemented with 0.1% Triton-X-100 [X100, Sigma-Aldrich] and 10% normal donkey serum [017-000-121, Jackson ImmunoResearch]) for at least one hour at RT. After blocking, cells were stained with rabbit-anti-Vimentin antibody (EPR3776, Abcam) diluted 1:1000 in blocking solution overnight at 4°C. After washing three times with PBS, a donkey-anti-rabbit Alexa Flour 488 antibody (AB_2313584, Jackson ImmunoResearch) was added in a dilution of 1:500 in blocking solution. Wells were washed again with PBS and incubated in DAPI stain (1:10,000) for 10 min. Coverslips were washed again in PBS and mounted onto slides with Eukitt quick-hardening mounting medium (03989, Sigma-aldrich). Slides were dried overnight before picture caption using an Olympus CKX53 and cellSens software (Olympus). Percentage of vimentin-positive cells was determined using Fiji cell counter plugin (Schindelin et al. 2012).

Primary Sertoli cell culture

24-well plates were coated with a DSA-lectin (L2766, Sigma Aldrich) solution (5 µg/ml in 1x Hank's balanced salt solution [HBSS, Gibco]) for at least 1 hour at 37°C. Plates were washed twice with 1xHBSS before use. PND14 testes were enzymatically digested and resuspended in medium (DMEM high glucose [Sigma] supplemented with 0.1% bovine serum albumin [BSA, Sigma], 1x GlutaMAX [Gibco], 1x Minimum Essential Medium Non-essential Amino Acids [Gibco] and 1% Pen-Strep) at 800,000 cells/ml. 500 µl of cell suspension were added

to DSA-lectin coated 24-wells and cells were allowed to attach for 2 hours at 32°C. Cells were incubated with a hypotonic solution (0.3xHBSS) for 1-2 minutes at RT to remove germ cells, washed with 1xHBSS to eliminate debris and new medium was added. Cells were left undisturbed for 24 hours before treatment.

Serum treatment of primary Sertoli cell cultures

Cell culture medium was supplemented with 10% serum from MSUS and control adult males (batch 1), sterile-filtered using 0.22 µm PVDF filter units (Merck) and distributed to each well by individual male (1 well/mouse). After 24 hours, medium was removed and used for lactate/pyruvate assessment or snap-frozen and stored at -80°C. Cells were washed once with 1xPBS and harvested in 500 µl TRIzol (Thermo Fisher Scientific) for RNA extraction. This experiment was conducted twice in independent replicates.

Lactate/pyruvate assessment

Conditioned medium was centrifuged at 3,200xg for 10 min at 4°C to remove debris and transferred to 10 kDa spin columns (Amicon Ultra, Merck). Proteins that may influence lactate and pyruvate level were removed from the <10 kDa flow-through containing metabolites by centrifugation at 14,000xg for 25 min at 4°C. Lactate and pyruvate were measured in the protein-depleted flow-through using assay kits (MAK064-1KT, Sigma-Aldrich) and (ab65342, Abcam) according to the manufacturer's instructions. Each sample was run twice and fluorescence was measured on a NOVOStar Microplate reader (BMG Labtech) and averaged. For each sample, lactate/pyruvate ratio was calculated using the average lactate and pyruvate measurements of the replicates.

ROS assessment

ROS production was measured in serum-treated primary Sertoli cultures using DCFDA/H2DCFDA-Cellular ROS Assay Kit (ab113851, Abcam) according to the manufacturer's instructions. Fluorescence was measured immediately, then after 10, 30, and

60 minutes on a NOVOStar Microplate reader (BMG Labtech). The experiment was run in triplicates, which were averaged for each time point.

RNA and DNA extraction

For sorted Sertoli cells obtained from adult males, RNA and DNA were extracted using the AllPrep DNA/RNA/miRNA Universal Kit (Qiagen) according to the manufacturer's instructions. For cultured cells harvested in TRIzol (Thermo Fisher Scientific), a phenol/chloroform extraction method was used to prepare RNA.

RNA sequencing

RNA samples were run on a Bioanalyzer (Agilent) at a concentration of 1.5 ng/µl using the eukaryote total RNA pico series II assay (Agilent) to assess RNA integrity. Libraries for RNA sequencing were prepared from 5 ng RNA/sample using the SMARTer Stranded Total RNA-Seq Kit v2 - Pico Input Mammalian (Takara) according to the manufacturer's instructions using 12 PCR cycles for amplification. DNA concentration of libraries was determined using Qubit dsDNA HS Assay Kit, and libraries were diluted to 1.5 ng/µl, then run on a Bioanalyzer (Agilent) using the High Sensitivity DNA Assay Protocol (Agilent) for quality control. Libraries were sequenced on an Illumina NovaSeq instrument, single-end at 100 bp.

Analyses of RNA sequencing data

Fastq files were checked for quality using FastQC (v 0.11.9) (Andrews 2010) trimmed with Trimgalore (v 0.6.5) (Krueger 2012) and pseudo-mapped with Salmon (v 1.1.0) (Patro et al. 2017) using an index file created from the GENCODE annotation of transcripts (vM23) (Frankish et al. 2019). For differential gene expression analysis, counts were normalized using the TMM method (Robinson and Oshlack 2010) and transformed with the voom method of the limma R-Package (v 3.42.2) (Ritchie et al. 2015) for linear modelling. All genes with $p<0.05$ were used for functional enrichment analyses using the g:GOSt function of g:Profiler

(Raudvere et al. 2019), taking into account GO terms and KEGG pathways with 10-1000 annotated genes. GO terms were further simplified using Revigo (Supek et al. 2011).

Fluidigm RT-qPCR

RNA was reverse-transcribed with miScript II RT reagents (Qiagen) using HiFlex buffer according to the manufacturer's instructions. For high-throughput gene expression analyses, samples and primers (list of primers: S4 Table) were prepared for the Fluidigm BioMark™ HD System (Fluidigm) according to the manufacturer's protocol. Pre-amplified cDNA samples and primers were loaded onto a 96.96 dynamic array™ (primers were loaded in duplicates) and mixed using an IFC (integrated fluidic circuits) machine (Fluidigm). Ready chips were then placed into a Fluidigm Biomark™ HD System for RT-qPCR analyses.

Analyses of Fluidigm RT-qPCR data

Baseline correction (using linear derivative) and assessment of cycle threshold (Ct) values were performed by the BioMark HD software (Fluidigm). A list of Ct values was obtained from the BioMark output tables and ordered according to sample batch. ReadqPCR (v 1.32.0) and NormqPCR (v 1.32.0) were used for downstream data preparation, including combination of technical replicates, normalizing to the 2 most stable reference genes out of 5 (Actb, B2m, Hrpt1, Rplp0 or Vim), and deriving delta C_q values. Samples were normalized to the mean of control samples and log2 foldchanges were calculated.

Determination of mitochondrial copy number variation (CNV)

DNA samples were analyzed by RT-qPCR using QuantiTect SYBR (Qiagen) on a Light Cycler II 480 (Roche): 95°C for 15 min, 45 cycles of 15 sec at 94°C, 30 sec at 55°C and 30 sec at 70°C. HK2 primers amplifying nuclear DNA were used as endogenous control and ND1

492 primers to amplify mitochondrial DNA (Primers list in S4 Table). Fold change of ND1 versus
493 HK2 amplification was calculated with 2^(-delta delta CT) method and normalized to controls.

494 Statistics

495 Student's t-test was used to assess significance between two groups. Kenward-Roger method
496 using R packages lmerTest (v 3.1-3) and lme4 (v 1.1-27.1) was used to assess significance
497 for experiments run in duplicates. Outliers at a distance greater than 2.5 standard deviations
498 from 0 were removed before analyses.

499

500 Data availability

501 The RNA-sequencing datasets collected in this study are available in the Gene Expression
502 Omnibus GSE205330.

503

504 Acknowledgements

505 We thank Chiara Boscardin, Anastasia Efimova, Lola Kourouma, and Anar Alshanbayeva for
506 assisting with the mouse work including breeding and MSUS paradigm, Andrew McDonald,
507 Silvia Schelbert, and Alberto Corcoba for animal license and laboratory organization in Zürich,
508 and Yvonne Zipfel and Jerome Bürki for animal care in Zürich. We are grateful for the valuable
509 input from Pierre-Luc Germain and Deepak Kumar Tanwar for bioinformatic analyses, from
510 Ali Jawaid for general input on study and experimental design, and Maria Dimitriu, Nancy
511 Carullo, and Rodrigo Arzate-Mejia for proof reading. We are thankful to Niharika Obrist for
512 technical assistance and Tao Lei and Jörg Klug from the Institute of Anatomy and Cell Biology
513 at the University of Giessen, Germany for help with the protocol for Sertoli cell cultures. We
514 thank the team of the cytometry facility at the University of Zurich for all FACS related issues,
515 Aria Minder and Silvia Kobel of the Genomic Diversity Center for assistance with the fluidigm

qPCR, and the team of the Functional Genomics Center Zurich for assistance with RNA sequencing. This work was funded by the University of Zurich, the ETH Zurich, the National Centre of Competence in Research (NCCR) RNA & Disease funded by the Swiss National Science Foundation (grant number 182880/Phase 2 and 205601/Phase 3), ETH grants (ETH-10 15-2 and ETH-17 13-2), and the Escher Family Fund. Illustrations in figures 1a, 3a, and 4a as well as the graphical abstract were created with BioRender.com.

Author contributions

KMT and IMM conceived and designed the study, and wrote the manuscript. FM conducted MSUS treatment and prepared animals with the help of KMT. KMT collected and prepared Sertoli cells and serum for transcriptomic analyses and serum treatments of cell cultures. KMT prepared RNA libraries for RNA sequencing. KMT and SL prepared primary Sertoli cell cultures, and carried out serum treatment and molecular analyses. KMT analyzed the data and prepared the Figs. IMM provided conceptual support throughout the project, and raised funds to finance the project.

Conflict of interest

The authors declare no conflict of interest.

References

Andrews, S. 2010. “FastQC: A Quality Control Tool for High Throughput Sequence Data.” Available at: Http://Www.Bioinformatics.Babraham.Ac.Uk/Projects/Fastqc. 2010.

Anway, Matthew D., Janet Folmer, William W Wright, and Barry R Zirkin. 2003. “Isolation of Sertoli Cells from Adult Rat Testes: An Approach to Ex Vivo Studies of Sertoli Cell

Function." *Biology of Reproduction* 68 (3): 996–1002. https://doi.org/10.1095/biolreprod.102.008045.

Autengruber, A, M Gereke, G Hansen, C Hennig, and D Bruder. 2012. "Impact of Enzymatic Tissue Disintegration on the Level of Surface Molecule Expression and Immune Cell Function." *European Journal of Microbiology & Immunology* 2 (2): 112–20. https://doi.org/10.1556/EuJMI.2.2012.2.3.

Bereiter-Hahn, J, and M Vöth. 1994. "Dynamics of Mitochondria in Living Cells: Shape Changes, Dislocations, Fusion, and Fission of Mitochondria." *Microscopy Research and Technique* 27 (3): 198–219. https://doi.org/10.1002/jemt.1070270303.

Bhushan, Sudhanshu, Ferial Aslani, Zhengguo Zhang, Tim Sebastian, Hans-Peter Elsasser, and Jorg Klug. 2016. "Isolation of Sertoli Cells and Peritubular Cells from Rat Testes." *Journal of Visualized Experiments : JoVE*, no. 108 (February): e53389. https://doi.org/10.3791/53389.

Bräuner, Elvira V, Loa Nordkap, Lærke Priskorn, Åse Marie Hansen, Anne Kirstine Bang, Stine A Holmboe, Lone Schmidt, Tina K Jensen, and Niels Jørgensen. 2020. "Psychological Stress, Stressful Life Events, Male Factor Infertility, and Testicular Function: A Cross-Sectional Study." *Fertility and Sterility* 113 (4): 865–75. https://doi.org/10.1016/j.fertnstert.2019.12.013.

Clutton, Genevieve, Katie Mollan, Michael Hudgens, and Nilu Goonetilleke. 2019. "A Reproducible, Objective Method Using MitoTracker(R) Fluorescent Dyes to Assess Mitochondrial Mass in T Cells by Flow Cytometry." *Cytometry. Part A : The Journal of the International Society for Analytical Cytology* 95 (4): 450–56. https://doi.org/10.1002/cyto.a.23705.

Frankish, Adam, Mark Diekhans, Anne-Maud Ferreira, Rory Johnson, Irwin Jungreis, Jane Loveland, Jonathan M Mudge, et al. 2019. "GENCODE Reference Annotation for the Human and Mouse Genomes." *Nucleic Acids Research* 47 (D1): D766–73.

https://doi.org/10.1093/nar/gky955.

Franklin, Tamara B, Holger Russig, Isabelle C Weiss, Johannes Graff, Natacha Linder, Aubin Michalon, Sandor Vizi, and Isabelle M Mansuy. 2010. “Epigenetic Transmission of the Impact of Early Stress across Generations.” *Biological Psychiatry* 68 (5): 408–15.

Gapp, Katharina, Ali Jawaid, Peter Sarkies, Johannes Bohacek, Pawel Pelczar, Julien Prados, Laurent Farinelli, Eric Miska, and Isabelle M. Mansuy. 2014. “Implication of Sperm RNAs in Transgenerational Inheritance of the Effects of Early Trauma in Mice.” *Nature Neuroscience* 17: 667–669.

Gaysinskaya, Valeriya, Ina Y Soh, Godfried W van der Heijden, and Alex Bortvin. 2014. “Optimized Flow Cytometry Isolation of Murine Spermatocytes.” *Cytometry. Part A : The Journal of the International Society for Analytical Cytology* 85 (6): 556–65. https://doi.org/10.1002/cyto.a.22463.

Green, Christopher Daniel, Qianyi Ma, Gabriel L Manske, Adrienne Niederriter Shami, Xianing Zheng, Simone Marini, Lindsay Moritz, et al. 2018. “A Comprehensive Roadmap of Murine Spermatogenesis Defined by Single-Cell RNA-Seq.” *Developmental Cell* 46 (5): 651-667.e10. https://doi.org/10.1016/j.devcel.2018.07.025.

Griswold, Michael D. 2018. “50 Years of Spermatogenesis: Sertoli Cells and Their Interactions with Germ Cells.” *Biology of Reproduction* 99 (1): 87–100. https://doi.org/10.1093/biolre/ioy027.

Guerrero-Bosagna, Carlos, Marina Savenkova, Md Muksitul Haque, Eric Nilsson, and Michael K. Skinner. 2013. “Environmentally Induced Epigenetic Transgenerational Inheritance of Altered Sertoli Cell Transcriptome and Epigenome: Molecular Etiology of Male Infertility.” *PLoS ONE* 8 (3): e59922. https://doi.org/10.1371/journal.pone.0059922.

Kaur, Gurvinder, Kandis Wright, Payal Mital, Taylor Hibler, Jonathan M Miranda, Lea Ann Thompson, Katelyn Halley, and Jannette M Dufour. 2020. “Neonatal Pig Sertoli Cells

592 Survive Xenotransplantation by Creating an Immune Modulatory Environment Involving
593 CD4 and CD8 Regulatory T Cells." *Cell Transplantation* 29: 963689720947102.
594 https://doi.org/10.1177/0963689720947102.

595 Krueger, F. 2012. "Trim Galore: A Wrapper Tool around Cutadapt and FastQC to
596 Consistently Apply Quality and Adapter Trimming to FastQ Files, with Some Extra
597 Functionality for MspI-Digested RRBS-Type (Reduced Representation Bisufite-Seq)
598 Libraries." Available at: Https://Www.Bioinformatics.Babraham. 2012.

599 Luo, Dandan, Meijie Zhang, Xiaohui Su, Luna Liu, Xinli Zhou, Xiujuan Zhang, Dongmei
600 Zheng, Chunxiao Yu, and Qingbo Guan. 2020. "High Fat Diet Impairs Spermatogenesis
601 by Regulating Glucose and Lipid Metabolism in Sertoli Cells." *Life Sciences* 257
602 (September): 118028. https://doi.org/10.1016/j.lfs.2020.118028.

603 Mächler, Philipp, Matthias T Wyss, Maha Elsayed, Jillian Stobart, Robin Gutierrez,
604 Alexandra von Faber-Castell, Vincens Kaelin, et al. 2016. "In Vivo Evidence for a
605 Lactate Gradient from Astrocytes to Neurons." *Cell Metabolism* 23 (1): 94–102.
606 https://doi.org/10.1016/j.cmet.2015.10.010.

607 Mäkelä, Juho-Antti, and Robin M Hobbs. 2019. "Molecular Regulation of Spermatogonial
608 Stem Cell Renewal and Differentiation." *Reproduction (Cambridge, England)* 158 (5):
609 R169–87. https://doi.org/10.1530/REP-18-0476.

610 Mancuso, Francesca, Mario Calvitti, Domenico Milardi, Giuseppe Grande, Giulia Falabella,
611 Iva Arato, Stefano Giovagnoli, et al. 2018. "Testosterone and FSH Modulate Sertoli Cell
612 Extracellular Secretion: Proteomic Analysis." *Molecular and Cellular Endocrinology* 476
613 (November): 1–7. https://doi.org/10.1016/j.mce.2018.04.001.

614 Marreiros, Bruno C, Filipa Calisto, Paulo J Castro, Afonso M Duarte, Filipa V Sena, Andreia
615 F Silva, Filipe M Sousa, Miguel Teixeira, Patrícia N Refojo, and Manuela M Pereira.
616 2016. "Exploring Membrane Respiratory Chains." *Biochimica et Biophysica Acta* 1857
617 (8): 1039–67. https://doi.org/10.1016/j.bbabio.2016.03.028.

618 Miettinen, Teemu P, and Mikael Björklund. 2017. “Mitochondrial Function and Cell Size: An
619 Allometric Relationship.” *Trends in Cell Biology* 27 (6): 393–402.
620 https://doi.org/10.1016/j.tcb.2017.02.006.

621 Nolfi-Donegan, Deirdre, Andrea Braganza, and Sruti Shiva. 2020. “Mitochondrial Electron
622 Transport Chain: Oxidative Phosphorylation, Oxidant Production, and Methods of
623 Measurement.” *Redox Biology* 37 (October): 101674.
624 https://doi.org/10.1016/j.redox.2020.101674.

625 Oliveira, Vanessa Staldoni de, Allisson Jhonatan Gomes Castro, Juliana Tonietto
626 Domingues, Ariane Zamoner Pacheco de Souza, Débora da Luz Scheffer, Alexandra
627 Latini, Carlos Henrique Lemos Soares, Glen Van Der Kraak, and Fátima Regina Mena
628 Barreto Silva. 2020. “A Brazilian Pulp and Paper Mill Effluent Disrupts Energy
629 Metabolism in Immature Rat Testis and Alters Sertoli Cell Secretion and Mitochondrial
630 Activity.” *Animal Reproduction* 17 (2): e20190116. https://doi.org/10.1590/1984-3143-
631 AR2019-0116.

632 Patgiri, Anupam, Owen S. Skinner, Yusuke Miyazaki, Grigorij Schleifer, Eizo Marutani,
633 Hardik Shah, Rohit Sharma, et al. 2020. “An Engineered Enzyme That Targets
634 Circulating Lactate to Alleviate Intracellular NADH:NAD+ Imbalance.” *Nature*
635 *Biotechnology* 38 (3): 309–13. https://doi.org/10.1038/s41587-019-0377-7.

636 Patro, Rob, Geet Duggal, Michael I Love, Rafael A Irizarry, and Carl Kingsford. 2017.
637 “Salmon Provides Fast and Bias-Aware Quantification of Transcript Expression.” *Nature*
638 *Methods* 14 (4): 417–19. https://doi.org/10.1038/nmeth.4197.

639 Raudvere, Uku, Liis Kolberg, Ivan Kuzmin, Tambet Arak, Priit Adler, Hedi Peterson, and
640 Jaak Vilo. 2019. “G:Profiler: A Web Server for Functional Enrichment Analysis and
641 Conversions of Gene Lists (2019 Update).” *Nucleic Acids Research* 47 (W1): W191–
642 98. https://doi.org/10.1093/nar/gkz369.

643 Rebourcet, Diane, Junxi Wu, Lyndsey Cruickshanks, Sarah E Smith, Laura Milne,

644 Anuruddika Fernando, Robert J Wallace, et al. 2016. “Sertoli Cells Modulate Testicular
645 Vascular Network Development, Structure, and Function to Influence Circulating
646 Testosterone Concentrations in Adult Male Mice.” *Endocrinology* 157 (6): 2479–88.
647 https://doi.org/10.1210/en.2016-1156.

648 Regueira, Mariana, Agostina Gorga, Gustavo Marcelo Rindone, Eliana Herminia Pellizzari,
649 Selva Beatriz Cigorraga, Maria Noel Galardo, Maria Fernanda Riera, and Silvina
650 Beatriz Meroni. 2018. “Apoptotic Germ Cells Regulate Sertoli Cell Lipid Storage and
651 Fatty Acid Oxidation.” *Reproduction (Cambridge, England)* 156 (6): 515–25.
652 https://doi.org/10.1530/REP-18-0181.

653 Ritchie, Matthew E, Belinda Phipson, Di Wu, Yifang Hu, Charity W Law, Wei Shi, and
654 Gordon K Smyth. 2015. “Limma Powers Differential Expression Analyses for RNA-
655 Sequencing and Microarray Studies.” *Nucleic Acids Research* 43 (7): e47.
656 https://doi.org/10.1093/nar/gkv007.

657 Robinson, Mark D, and Alicia Oshlack. 2010. “A Scaling Normalization Method for
658 Differential Expression Analysis of RNA-Seq Data.” *Genome Biology* 11 (3): R25.
659 https://doi.org/10.1186/gb-2010-11-3-r25.

660 Rotgers, E, S Cisneros-Montalvo, K Jahnukainen, J Sandholm, J Toppari, and M Nurmio.
661 2015. “A Detailed Protocol for a Rapid Analysis of Testicular Cell Populations Using
662 Flow Cytometry.” *Andrology* 3 (5): 947–55. https://doi.org/10.1111/andr.12066.

663 Ruigrok, S R, K Yim, T L Emmerzaal, B Geenen, N Stöberl, J L den Blaauwen, M R Abbink,
664 et al. 2021. “Effects of Early-Life Stress on Peripheral and Central Mitochondria in Male
665 Mice across Ages.” *Psychoneuroendocrinology* 132 (October): 105346.
666 https://doi.org/10.1016/j.psyneuen.2021.105346.

667 Sadler-Riggleman, Ingrid, Rachel Klukovich, Eric Nilsson, Daniel Beck, Yeming Xie, Wei
668 Yan, and Michael K Skinner. 2019. “Epigenetic Transgenerational Inheritance of Testis
669 Pathology and Sertoli Cell Epimutations: Generational Origins of Male Infertility.”

Environmental Epigenetics 5 (3): dvz013. https://doi.org/10.1093/eep/dvz013.

Sajadi, Ensieh, Sara Dadras, Mohammad Bayat, Shabnam Abdi, Hamid Nazarian, Sanaz Ziaeipour, Fatemeh Mazini, et al. 2019. "Impaired Spermatogenesis Associated with Changes in Spatial Arrangement of Sertoli and Spermatogonial Cells Following Induced Diabetes." *Journal of Cellular Biochemistry* 120 (10): 17312–25. https://doi.org/10.1002/jcb.28995.

Sarkar, D, and S K Singh. 2017. "Neonatal Hypothyroidism Affects Testicular Glucose Homeostasis through Increased Oxidative Stress in Prepubertal Mice: Effects on GLUT3, GLUT8 and Cx43." *Andrology* 5 (4): 749–62. https://doi.org/10.1111/andr.12363.

Scarpino, Stefania, Anna Rita Morena, Cecilia Petersen, Berit Fröysa, Olle Söder, and Carla Boitani. 1998. "A Rapid Method of Sertoli Cell Isolation by DSA Lectin, Allowing Mitotic Analyses." *Molecular and Cellular Endocrinology* 146 (1–2): 121–27. https://doi.org/10.1016/S0303-7207(98)00190-7.

Schindelin, Johannes, Ignacio Arganda-Carreras, Erwin Frise, Verena Kaynig, Mark Longair, Tobias Pietzsch, Stephan Preibisch, et al. 2012. "Fiji: An Open-Source Platform for Biological-Image Analysis." *Nature Methods* 9 (7): 676–82. https://doi.org/10.1038/nmeth.2019.

Sharpe, Richard M, Chris McKinnell, Catrina Kivlin, and Jane S Fisher. 2003. "Proliferation and Functional Maturation of Sertoli Cells, and Their Relevance to Disorders of Testis Function in Adulthood." *Reproduction (Cambridge, England)* 125 (6): 769–84. https://doi.org/10.1530/rep.0.1250769.

Steenwyk, Gretchen van, Katharina Gapp, Ali Jawaid, Pierre-Luc Germain, Francesca Manuella, Deepak K Tanwar, Nicola Zamboni, et al. 2020. "Involvement of Circulating Factors in the Transmission of Paternal Experiences through the Germline." *The EMBO Journal* 39 (23): e104579. https://doi.org/10.15252/embj.2020104579.

696 Supek, Fran, Matko Bošnjak, Nives Škunca, and Tomislav Šmuc. 2011. “REVIGO
697 Summarizes and Visualizes Long Lists of Gene Ontology Terms.” *PloS One* 6 (7):
698 e21800. https://doi.org/10.1371/journal.pone.0021800.

699 Tian, Pengxiang, Zhiming Zhao, Yanli Fan, Na Cui, Baojun Shi, and Guimin Hao. 2021.
700 “Changes in Expressions of Spermatogenic Marker Genes and Spermatogenic Cell
701 Population Caused by Stress.” *Frontiers in Endocrinology* 12: 584125.
702 https://doi.org/10.3389/fendo.2021.584125.

703 Titov, Denis V, Valentin Cracan, Russell P Goodman, Jun Peng, Zenon Grabarek, and
704 Vamsi K Mootha. 2016. “Complementation of Mitochondrial Electron Transport Chain
705 by Manipulation of the NAD+/NADH Ratio.” *Science (New York, N.Y.)* 352 (6282):
706 231–35. https://doi.org/10.1126/science.aad4017.

707 Tsuji, Kunikazu, Miyoko Ojima, Koji Otabe, Masafumi Horie, Hideyuki Koga, Ichiro Sekiya,
708 and Takeshi Muneta. 2017. “Effects of Different Cell-Detaching Methods on the Viability
709 and Cell Surface Antigen Expression of Synovial Mesenchymal Stem Cells.” *Cell*
710 *Transplantation* 26 (6): 1089–1102. https://doi.org/10.3727/096368917X694831.

711 Wagle, J R, J J Heindel, A Steinberger, and B M Sanborn. 1986. “Effect of Hypotonic
712 Treatment on Sertoli Cell Purity and Function in Culture.” *In Vitro Cellular &*
713 *Developmental Biology : Journal of the Tissue Culture Association* 22 (6): 325–31.
714 https://doi.org/10.1007/BF02623406.

715 Wong, Wah J, and Yusuf S Khan. 2021. “Histology, Sertoli Cell.” In . Treasure Island (FL).

716 Zhang, Li-Li, Jing Ma, Bo Yang, Jie Zhao, Bin-Yuan Yan, Yuan-Qiang Zhang, and Wei Li.
717 2018. “Interference with Lactate Metabolism by Mmu-MiR-320-3p via Negatively
718 Regulating GLUT3 Signaling in Mouse Sertoli Cells.” *Cell Death & Disease* 9 (10): 964.
719 https://doi.org/10.1038/s41419-018-0958-2.

720 Zimmermann, Celine, Isabelle Stevant, Christelle Borel, Beatrice Conne, Jean-Luc Pitetti,
721 Pierre Calvel, Henrik Kaessmann, Bernard Jegou, Frederic Chalmel, and Serge Nef.

722 2015. “Research Resource: The Dynamic Transcriptional Profile of Sertoli Cells during
723 the Progression of Spermatogenesis.” *Molecular Endocrinology (Baltimore, Md.)* 29 (4):
724 627–42. https://doi.org/10.1210/me.2014-1356.

725 Zomer, Helena D, and Prabhakara P Reddi. 2020a. “Characterization of Rodent Sertoli Cell
726 Primary Cultures.” *Molecular Reproduction and Development* 87 (8): 857–70.
727 https://doi.org/10.1002/mrd.23402.

728 ———. 2020b. “Mouse Sertoli Cells Isolation by Lineage Tracing and Sorting.” *Molecular*
729 *Reproduction and Development* 87 (8): 871–79. https://doi.org/10.1002/mrd.23406.

730

731

Supporting information

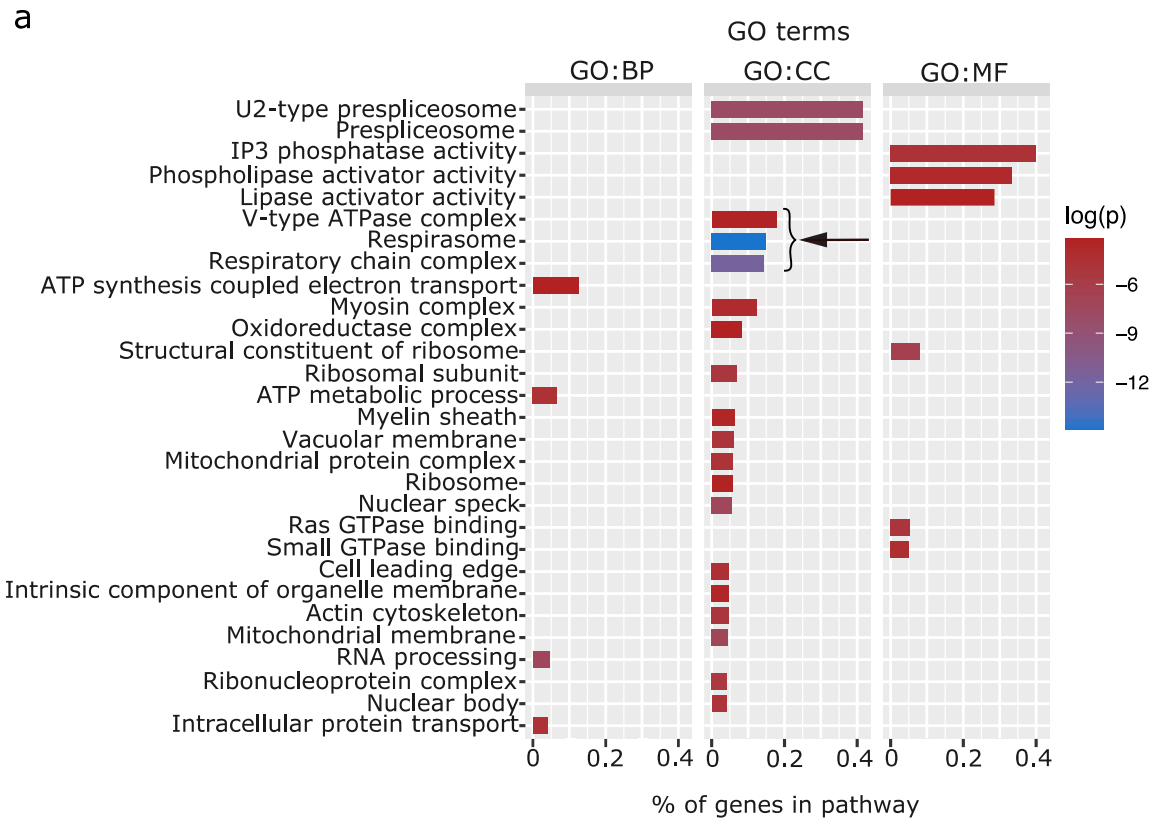

S1 Fig. Enriched GO terms of altered genes in MSUS Sertoli cells. (a) Enriched GO pathways of significantly altered genes ($p<0.05$) in MSUS mouse Sertoli cells detected by RNA sequencing. Ratio of genes per pathway is given on the x-axis and log of p-value (log(p)) is indicated on a color scale. Bracket and arrow indicate mitochondrially related pathways. BP: biological process; CC: cellular component; MF: molecular function

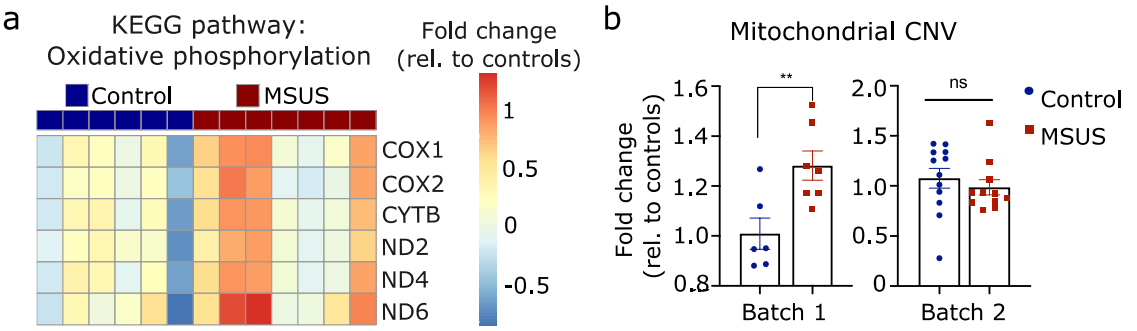

741

742 **S2 Fig. High variability in mitochondrially encoded genes and mitochondrial CNV in**
743 **batch 1 Sertoli cells.** (a) Heatmap of altered mitochondrially encoded genes of KEGG
744 pathway "oxidative phosphorylation". Fold change relative to controls is indicated in the color
745 scale. (b) Fold changes in mitochondrial CNV of MSUS compared to control Sertoli cells of
746 mouse batches 1 and 2. Error bars: mean ± SEM; ** = p<0.01, student's t-test.

747

748

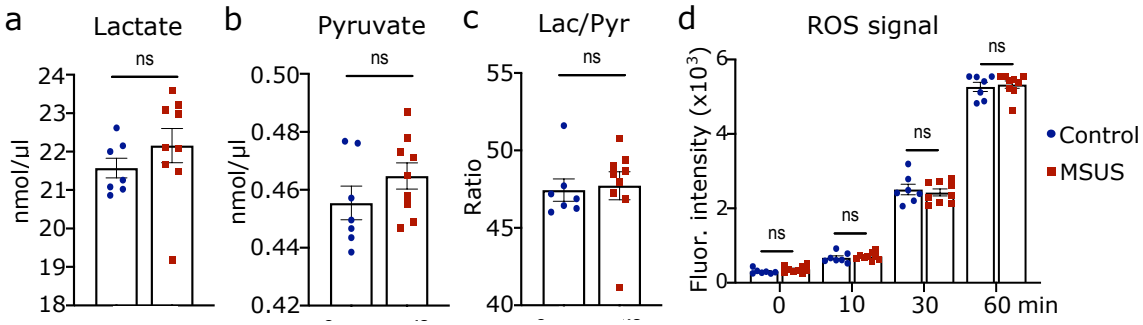

749

750 **S3 Fig. Characterization of lactate-to-pyruvate ratio and ROS production after MSUS**
751 **serum exposure in primary Sertoli cells.** (a) Lactate and (b) pyruvate levels (in nmol/µl) in
752 primary Sertoli cell medium after 24h of serum exposure. (c) Ratio of lactate to pyruvate and
753 (d) ROS fluorescent signal in primary Sertoli cells after serum exposure. Controls, n=7; MSUS,
754 n=9 for all graphs; error bars: mean ± SEM; ns=not significant, student's t-test.

755

A

RAW COUNTS	Before		Haploid		Diploid		Tetraploid		highFSC		lowFSC		highAPC		lowAPC	
	VIM	DAPI	VIM	DAPI	VIM	DAPI	VIM	DAPI	VIM	DAPI	VIM	DAPI	VIM	DAPI	VIM	DAPI
Replicate 1.1	1	28	0	34	7	32	1	17	13	31	0	25	10	11	1	9
Replicate 1.2	0	18	0	25	3	15	0	50	5	21	1	15	5	6	0	10
Replicate 1.3	0	23	0	12	1	20	2	60	6	19	3	40	5	7	0	10
Replicate 1.4													5	6	0	17
Replicate 1.5													10	12	0	13
Replicate 1.6													9	10		
Replicate 2.1	0	20	0	16	1	10	1	16	27	31	0	29	53	56	1	33
Replicate 2.2	1	21	0	23	3	31	0	22	13	16	0	23	44	46	1	25
Replicate 2.3	0	23	0	13	3	11	0	33	13	16	2	12	26	28	0	19
Replicate 2.4					2	10					1	23				
Replicate 3.1	0	38	0	19	3	19	0	41	4	28	0	32	9	10	2	29
Replicate 3.2	1	36	0	13	3	19	2	50	5	15	1	26	6	8	0	16
Replicate 3.3	1	48	0	13	2	14	1	61	2	9	0	29	10	11		
Replicate 3.4			0	48	9	41			3	17	1	29	24	30	1	22
Replicate 3.5									5	20			12	13		
Replicate 4.1	1	31	0	12	2	20	0	63	3	17	1	36	15	17	0	24
Replicate 4.2	1	21	0	13	4	26	1	64	2	15	3	41	16	18		
Replicate 4.3	1	28	0	15	2	31	0	36	1	10	3	21	16	18	1	15
Replicate 4.4	0	29	0	14	2	19			1	8			16	17	0	23

B

#CELLS COUNTED	Before	Haploid	Diploid	Tetrapl.	highFSC	lowFSC	highAPC	lowAPC
Replicate 1	69	71	67	127	71	80	52	59
Replicate 2	64	52	62	71	63	87	130	77
Replicate 3	122	93	93	152	89	116	72	67
Replicate 4	109	54	96	163	50	98	70	62
TOTAL	**364**	**270**	**318**	**513**	**273**	**381**	**324**	**265**

C

PERCENTAGES	Before	Haploid	Diploid	Tetrapl.	highFSC	lowFSC	highAPC	lowAPC
Replicate 1	0.014	0.000	0.164	0.024	0.338	0.050	0.846	0.017
Replicate 2	0.016	0.000	0.145	0.014	0.841	0.034	0.946	0.026
Replicate 3	0.016	0.000	0.183	0.020	0.213	0.017	0.847	0.045
Replicate 4	0.028	0.000	0.104	0.006	0.140	0.071	0.900	0.016
weighted Averag	**0.0192**	**0.0000**	**0.1478**	**0.0156**	**0.3773**	**0.0420**	**0.8981**	**0.0264**
weighted SD	0.0063	0.0000	0.0363	0.0081	0.3036	0.0241	0.0508	0.0132

S1 Table. Counts of vimentin-positive cells in isolated FACS populations. (A) Raw counts of each isolated fraction (before FACS, haploid, diploid, tetraploid, high FSC, low FSC, high APC and low APC) for 4 individual mice (4 replicates). Always at least 3 individual pictures per replicate were taken and counted. (B) Total number of cells counted for each replicate and each isolated fraction. (C) Percentages of vimentin positive cells out of all DAPI positive cells for each replicate and isolated fraction. Weighted average and weighted standard deviation (SD) were calculated from percentages.

Source	Term name	Term ID	Adj. P-value
KEGG	Oxidative phosphorylation	KEGG:00190	1.08E-08
GO:CC	respirasome	GO:0070469	3.40E-07
WP	Electron Transport Chain	WP:WP295	6.54E-07
GO:CC	respiratory chain complex	GO:0098803	7.44E-06
GO:CC	mitochondrial respirasome	GO:0005746	5.50E-05
HP	Atrophy/Degeneration affecting the cerebrum	HP:0007369	0.00025262
KEGG	Parkinson disease	KEGG:05012	0.00025719
GO:CC	prespliceosome	GO:0071010	0.00035071
GO:CC	U2-type prespliceosome	GO:0071004	0.00035071
HP	Protruding ear	HP:0000411	0.00040705
HP	Cerebral atrophy	HP:0002059	0.00048261
GO:CC	nuclear speck	GO:0016607	0.00070203
HP	Centrocecal scotoma	HP:0000576	0.00070315
HP	Brain atrophy	HP:0012444	0.00071712
GO:BP	RNA processing	GO:0006396	0.00075713
GO:CC	mitochondrial membrane	GO:0031966	0.00084584
KEGG	Non-alcoholic fatty liver disease (NAFLD)	KEGG:04932	0.00096033
KEGG	Thermogenesis	KEGG:04714	0.00140948
REAC	NMD independent of the Exon Junction Complex (EJC)	REAC:R-MMU-975956	0.00180478
GO:MF	structural constituent of ribosome	GO:0003735	0.00184033
HP	Ventricular preexcitation	HP:0004309	0.00292897
REAC	Golgi Associated Vesicle Biogenesis	REAC:R-MMU-432722	0.00323917
HP	Stroke-like episode	HP:0002401	0.00353918
KEGG	Huntington disease	KEGG:05016	0.00361302
GO:CC	mitochondrial envelope	GO:0005740	0.00380836
HP	Atrophy/Degeneration affecting the central nervous system	HP:0007367	0.00387525
HP	Hemianopia	HP:0012377	0.00403308
GO:CC	ribonucleoprotein complex	GO:1990904	0.00446442
GO:CC	mitochondrial inner membrane	GO:0005743	0.00466444
GO:CC	ribosomal subunit	GO:0044391	0.00525599
HP	Episodic vomiting	HP:0002572	0.00565689
GO:MF	Ras GTPase binding	GO:0017016	0.00675107
GO:CC	actin cytoskeleton	GO:0015629	0.00686765
HP	Leber optic atrophy	HP:0001112	0.00691632
GO:CC	vacuolar membrane	GO:0005774	0.00697451
GO:CC	nuclear body	GO:0016604	0.00724207
GO:CC	inner mitochondrial membrane protein complex	GO:0098800	0.00751333
GO:CC	mitochondrial protein complex	GO:0098798	0.0079944
HP	Generalized-onset seizure	HP:0002197	0.00809124
KEGG	Ribosome	KEGG:03010	0.00861026
HP	Abnormal facial expression	HP:0005346	0.00870291
GO:MF	inositol trisphosphate phosphatase activity	GO:0046030	0.00895213
REAC	SRP-dependent cotranslational protein targeting to membrane	REAC:R-MMU-1799339	0.00933222
WP	Cytoplasmic Ribosomal Proteins	WP:WP163	0.01034732
GO:BP	intracellular protein transport	GO:0006886	0.01035823
GO:CC	cytosolic ribosome	GO:0022626	0.01051453
GO:BP	ATP metabolic process	GO:0046034	0.01086537
HP	Decreased facial expression	HP:0004673	0.01095364
GO:CC	organelle inner membrane	GO:0019866	0.0113213
GO:CC	cell leading edge	GO:0031252	0.01132506
HP	Retinal telangiectasia	HP:0007763	0.01219897
HP	Wolff-Parkinson-White syndrome	HP:0001716	0.01219897
HP	Mitochondrial respiratory chain defects	HP:0200125	0.01219897
HP	Central retinal vessel vascular tortuosity	HP:0007768	0.01237967
HP	Retinal arterial tortuosity	HP:0000631	0.01237967
REAC	NMD enhanced by the Exon Junction Complex (EJC)	REAC:R-MMU-975957	0.01327594
REAC	Nonsense-Mediated Decay (NMD)	REAC:R-MMU-927802	0.01327594
GO:MF	small GTPase binding	GO:0031267	0.01330476
GO:CC	myosin complex	GO:0016459	0.0185582
HP	Abnormal cerebellum morphology	HP:0001317	0.02010541
GO:MF	phospholipase activator activity	GO:0016004	0.02050276
HP	Psychotic episodes	HP:0000725	0.02072004
GO:CC	lysosomal membrane	GO:0005765	0.02121812
GO:CC	lytic vacuole membrane	GO:0098852	0.02121812
REAC	Formation of a pool of free 40S subunits	REAC:R-MMU-72689	0.02157739
TF	Factor: HIF2A; motif: NTACGTGMN	TF:M10221	0.02244509
TF	Factor: HIF2A; motif: NTACGTGMN; match class: 0	TF:M10221_0	0.02244509
HP	Abnormality of hindbrain morphology	HP:0011282	0.02306827
HP	Abnormality of the metencephalon	HP:0011283	0.02306827
HP	Arterial tortuosity	HP:0005116	0.02425621
WP	Oxidative phosphorylation	WP:WP1248	0.02791317
REAC	trans-Golgi Network Vesicle Budding	REAC:R-MMU-199992	0.02794761
HP	Mitochondrial inheritance	HP:0001427	0.02868439
HP	Abnormal adipose tissue morphology	HP:0009124	0.02908822
REAC	Membrane Trafficking	REAC:R-MMU-199991	0.02950059
GO:CC	myelin sheath	GO:0043209	0.02989145
GO:CC	large ribosomal subunit	GO:0015934	0.03002648
GO:CC	intrinsic component of organelle membrane	GO:0031300	0.03046085
HP	Vascular tortuosity	HP:0004948	0.03313985
GO:CC	proton-transporting V-type ATPase complex	GO:0033176	0.03442199
HP	Ragged-red muscle fibers	HP:0003200	0.03526572
GO:CC	ribosome	GO:0005840	0.03672133
REAC	Translation	REAC:R-MMU-72766	0.03678056
GO:MF	lipase activator activity	GO:0060229	0.04028618
GO:BP	ATP synthesis coupled electron transport	GO:0042773	0.04076191
GO:CC	oxidoreductase complex	GO:1990204	0.0409364
HP	Aplasia/Hypoplasia of the cerebellum	HP:0007360	0.04094948
GO:CC	cytosolic large ribosomal subunit	GO:0022625	0.04326678
HP	Developmental cataract	HP:0000519	0.04328818
REAC	The citric acid (TCA) cycle and respiratory electron transport	REAC:R-MMU-1428517	0.04505193
KEGG	Alzheimer disease	KEGG:05010	0.04541879
REAC	L13a-mediated translational silencing of Ceruloplasmin expression	REAC:R-MMU-156827	0.04912657

S2 Table. Summary of the over-representation analyses of significantly altered genes. All significantly altered genes ($p<0.05$) in response to MSUS were used for over-representation analyses using Gprofiler. The table shows the source, term name, term ID and adjusted p-value for each significant pathway.

769

A	Number	Group	Cage	Littercage
	1	MSUS	11	576
	5	MSUS	15	606
	6	MSUS	15	589
	9	CTRL	3	577
	10	CTRL	3	583
	11	MSUS	17	589
	12	CTRL	3	590
	13	MSUS	17	608
	14	CTRL	3	601
	22	CTRL	6	580
	23	MSUS	20	600
	24	CTRL	6	583
	26	MSUS	20	597

B	Number	Group	Cage	Littercage
	1	Control	50	6
	2	MSUS	57	7
	3	Control	50	18
	9	MSUS	61	8
	10	Control	42	1
	11	MSUS	61	21
	17	Control	51	6
	18	MSUS	62	8
	19	Control	51	27
	25	MSUS	59	7
	26	Control	45	1
	27	MSUS	59	19
	33	Control	48	2
	34	MSUS	58	7
	35	Control	48	18
	41	MSUS	54	4
	42	Control	43	1
	43	MSUS	54	16
	49	Control	47	2
	50	MSUS	55	4
	51	Control	47	18
	57	MSUS	56	7
	58	Control	44	1
	59	MSUS	56	16

C	Number	Group	Cage	Littercage
	9	CTRL	3	577
	10	CTRL	3	583
	11	MSUS	17	589
	12	CTRL	3	590
	13	MSUS	17	608
	14	CTRL	3	601
	15	MSUS	17	578
	16	CTRL	6	596
	17	MSUS	17	581
	18	MSUS	13	576
	19	MSUS	13	579
	20	MSUS	13	588
	21	MSUS	13	606
	22	CTRL	6	580
	23	MSUS	20	600
	24	CTRL	6	583

770

771 **S3 Table. Information on mice used for experiments.** (A) Mice used for RNA sequencing
772 of Sertoli cells (Batch 1). (B) Mice used for Fluidigm RT-qPCR of Sertoli cells (Batch 2). (C)
773 Mice used for serum collection for in vitro experiments. The tables contain information on the
774 number (ID), group, cage, and litter cage.

775

Gene	primer_fw_sequence	primer_rev_sequence
Actb	ACAGCTTCTTTGCAGCTCCTTCG	ATCGTCATCCATGGCGAACTGGTG
Atp5f1	AAGTGCGTCTTGGGCTGATTC	AAGCACATAAGGTCCTGTTACACC
Atp6ap1	AGGCAATCTCCTTGTGACCAACG	TCACATTGAAGGCCTGGATCTGG
Atp6v1a	TGTCGGATATCAGCAGTCAGACC	CACCAGTGATATGACTACCAACCC
Atpv0c	ACGAACAGCCTGACACATGCAC	ACAATGGGCACTAGGACACTGC
B2m	ACATACGCCTGCAGAGTTAAGC	TGCTTGATCACATGTCTCGATCCC
COX1	AAAGCCCACTTCGCCATCATATTC	AGCATCTGGGTAGTCTGAGTAGCG
COX2	AACCGAGTCGTTCTGCCAATAG	TGATTTAGTCGGCCTGGGATGG
Cox4i1	TGAGCCTGATTGGCAAGAGAGC	ACTCTTCACAACACTCCCATGTGC
Cox5a	CTGCATTGCGAGCATGTAGACG	GGTCCTGCTTTGTCCTTAACAACC
Cox6a1	TCCGACCGGCTATGAAGATGAG	AACCAGTGCTGTGGTCCCTTTG
CYTB	ACAAAGCCACCTTGACCCGATTC	GCTAGGGCCGCGATAATAAATGG
Hprt1	GCGTCGTGATTAGCGATGATGAAC	CGAGCAAGTCTTTCAGTCCTGTCC
ND2	TGATTACTTCTGCCAGCCTGACC	CGGTTTGTTTCTGCTAGGGTTGAG
ND4	GCACATGGCCTCACATCATCAC	GCTGTGGATCCGTTCGTAGTTG
ND6	GTTATGTTGGAAGGAGGGATTGGG	CGCAAACAAAGATCACCCAGCTAC
Ndufa1	CAATCGCTACTATGTGTCCAAGGG	GCCTTCTAACAGGAACAGATGACC
Ndufa9	TCTAAGTCCTTGAGGAGCAAGGC	ACGGCCGTATGATGATGGCTTC
Ppa2	TGACAAGGGAGCCATCAGTTGTG	AGTGCAGTGGAAAGGGCTATCG
Sdhc	ACTGAATGGGATCCGACACTTGC	ACAACACAGCAAGAACCACGAC
Sdhd	TCTGGTTCCAAGGCTGCATCTC	CCAAGAGCAGAACACTGACAACCC
Uqcr11	TCTGCACATGCGTAGTGCTC	GGCTGTGGGAATCCAGTTTCTG
HK2	GCCAGCCTCTCCTGATTTTAG	GGGAACACAAAAGACCTCTTC
ND1	CTAGCAGAAACAAACCGGGC	CCGGCTGCGTATTCTACGTT

776

777 **S4 Table. List of primer sequences.** The table includes information on the target genes,

778 forward primer and reverse primer sequences.

779